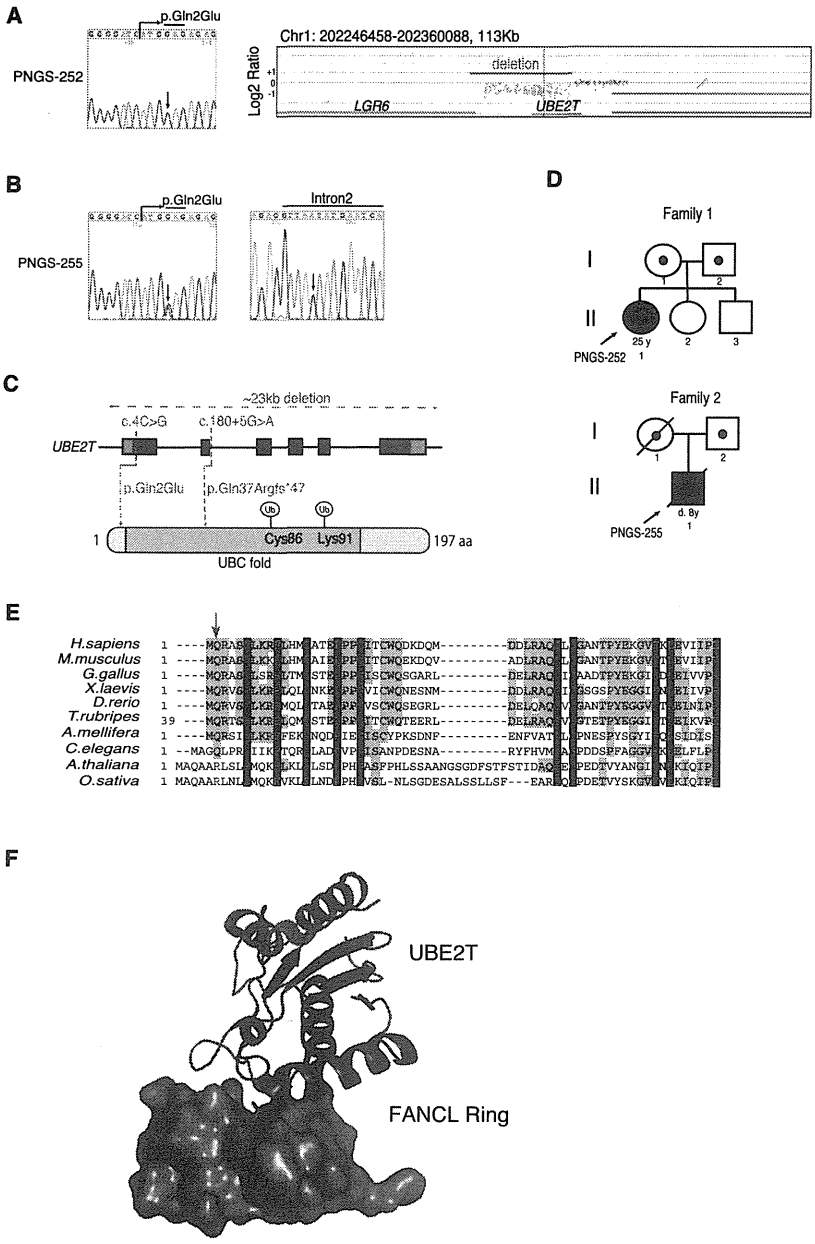

Figure 1. Identification of *UBE2T* Mutations

(A–C) Results of Sanger sequencing or array CGH of the individuals PNGS-252 (A) and PNGS-255 (B). In the array CGH, one of the deletion junctions was outside of our probes installed, and therefore it is impossible to see the whole deletion. A red line indicates the approximate region of the genome deletion detected by genome PCR (Figure S2). Schematic summary shown in (C).

Genomic DNA was isolated from PHA-stimulated lymphocytes via a Puregene (QIAGEN) kit. Genomic PCR was carried out using KOD-FX polymerase (TOYOBO) with primer pairs indicated in Table S1 and directly sequenced after ExoSAP-IT (Affymetrix) treatment or after purification from an agarose gel (Nucleospin, Takara). A custom CGH 4x180K array with a total of 179,673 50-mer probes in triplicate was designed using SureDesign (Agilent Technologies). The probes covered all of the known 16 genes associated with FA (including *FANCM* at the time of manufacturing) and related genes including *UBE2T*, *NBS1*, four *RAD51* paralogs, *FAAP20*, *FAAP24*, and *FAAP100*. Appropriate control probes were also included based on the recommendations from Agilent Technologies. After CGH slides were manufactured by Agilent Technologies, fluorochrome labeling of genomic DNA from the FA-affected individuals and the reference subjects, hybridization with the CGH slides, scanning, and preliminary analysis were done by Takara Bio company. Further analysis was carried out using Genomic workbench software (Agilent). Cys86 in UBE2T is the ubiquitin acceptor site, and Lys91 is an auto-ubiquitination site.

(D) Pedigrees of the probands' families.

(E) Alignments of the N-terminal UBE2T amino acid sequences across species. The following UBE2T amino acid sequences were aligned using Genetyx-Mac software with manual modifications (GenBank accession numbers shown): *H. sapiens*, NP_054895.3; *M. musculus*, NP_080300.1; *G. gallus*, XP_419230.2; *X. laevis*, NP_001080105.1; *D. rerio*, NP_001070763.1; *T. rubripes*, XP_003963365.2; *A. mellifera*, XP_003249077.1; *C. elegans*, NP_500272.2 ; *A. thaliana*, NP_566751.1; *O. sativa*, NP_001043518.1. The arrow indicates the Gln2 residue.

(F) Structure of the human FANCL Ring domain-UBE2T complex cited from Hodson et al.[15] The Gln2 residue is highlighted by red lines.

Variation Browser databases. The glutamine residue (Gln2) is highly conserved in the homologs found from vertebrates to worms excluding plants (Figure 1E) and the mutation is rated as "damaging" by both SIFT and PolyPhen predictions. The Gln2 is located in the N-terminal helix of UBE2T, which constitutes part of the hydrophobic E3-E2 interaction surface, near the conserved E2 UBC fold[15] (Figures 1C and 1F). Copy-number analysis using WES data suggested that there was a heterozygous deletion across the *UBE2T* locus in the PNGS-252 sample (data not shown). Indeed, our targeted array comparative genome hybridization (array CGH) revealed an area of reduced hybridization signal encompassing almost the entire *UBE2T* (Figure 1A). The deletion junction carried 3 bp of microhomology (Figures S2A–S2D), suggesting that the junction arose from microhomology-mediated repair.[17] This person's father carried the genomic deletion, and the mother had the heterozygous c.4C>G mutation (Figure S3). There was no family history of malformations, hematological abnormalities, or cancer predisposition.

In the individual PNGS-255, WES revealed the c.4C>G mutation as well as a splice donor site mutation

Table 1. Clinical Features of the Two FA-Affected Case Subjects

Individual	PNGS-252	PNGS-255
Sex	female	male
Age at BMF (year)[a]	7	3
First allele	c.4C>G (p.Gln2Glu)	c.4C>G (p.Gln2Glu)
Second allele	~23 kb deletion (g.202288583_202309772del)	c.180+5G>A (p.Gln37Argfs*47)
Physical abnormalities	left hypoplastic thumb, abnormalities of external genitalia, short stature	bilateral thumb polydactyly, abnormal shape of left ear, dysplasia of middle ear bone, deafness, facial nerve palsy
Hematological abnormalities	severe aplastic anemia	MDS (refractory anemia) evolving to AML
Age at HSCT (year)[b]	13	8
Outcome	alive and well 12 years after HSCT	died 5 months after HSCT
Solid tumors	none	none
Cells from JCRB Cell Bank	AP65P fibroblasts	not available
ALDH2 genotype	GA heterozygous	GA heterozygous

[a]The onset of BMF was defined as described.[16]
[b]Haematopoietic stem cell transplantation.

(c.180+5G>A) (Figures 1B and 1C). Both alterations were heterozygous and on different chromosomes (Figure S4). Thus, this individual was compound heterozygous for the *UBE2T* mutations. In bone marrow fibroblasts, we found a small fraction of *UBE2T* transcripts with skipped exon 2, resulting in a frameshift and premature stop codon (p.Gln37Argfs*47) (Figure S5). Family members of this person were not available for further evaluation. However, the results of SNP array analysis using the HumanOMni5 v.1.0 array (Illumina) suggested that a haplotype containing the c.4C>G mutation was shared by PNGS-252, her mother, and PNGS-255 (not shown). Thus, they might have a common ancestral origin.

We extended WES to AP65P FA fibroblasts provided by the JCRB Cell Bank and found the same *UBE2T* c.4C>G mutation. Moreover, 99.9% of the SNPs listed in dbSNP131 and identified in AP65P were identical to those in PNGS-252 (2,244 out of 2,247), demonstrating that AP65P was derived from PNGS-252 (Table 1). The AP65P individual has been reported as carrying no mutations in *FANCA*, *FANCG*, and *FANCC*.[18] We transformed the cells with human *TERT* (*hTERT*) and termed them AP65P-hTERT. Unfortunately, we were unable to immortalize bone marrow fibroblasts from PNGS-255.

Interestingly, AP65P-hTERT cells displayed roughly similar protein levels of UBE2T as normal control cells (48BR), indicating that the p.Gln2Glu substitution does not significantly destabilize UBE2T protein (Figure 2A). We also detected the auto-monoubiquitinated form of UBE2T as previously described,[7,8] suggesting that the mutant protein is able to receive activated ubiquitin from the E1 enzyme (Figure 2A). However, only faint amounts of long-form ID proteins were observed, even after MMC stimulation (Figure 2A). As expected, AP65P-hTERT cells transduced with lentivirus encoding normal UBE2T, but not with the mutant, clearly restored the MMC-induced long form of FANCD2 (Figure 2A) as well as FANCD2 foci formation (Figure 2B). Furthermore, both the increased levels of MMC-induced chromosome breakage (Figure 2C) and the MMC sensitivity (Figure 3A) in AP65P-hTERT cells were suppressed by exogenous wild-type UBE2T but not with UBE2T carrying p.Gln2Glu. Taken together, these results firmly established that the FA phenotype in these individuals is caused by the *UBE2T* mutations.

How, exactly, does the UBE2T alteration affect the activity of the protein in promoting monoubiquitination of the ID complex? We hypothesized that the p.Gln2Glu substitution might disrupt the FANCL-UBE2T interaction. Indeed, the p.Gln2Glu alteration drastically reduced the signal intensity in a mammalian two-hybrid assay (Figure 4A). This was confirmed by a GST pull-down experiment using purified recombinant human or chicken GST-FANCL and wild-type or mutant UBE2T proteins (Figure 4B, 4C, and S6A). In an in vitro monoubiquitination assay,[11] the mutated UBE2T protein displayed ~3-fold less efficiency in promoting FANCD2 monoubiquitination in the presence (Figure 4D) or absence (Figure S6B) of stimulator DNA, whereas auto-ubiquitination was normal compared to control proteins (Figure S6C). The p.Gln2Glu substitution abrogated FANCL monoubiquitination in vitro (Figures 4D, S6B, and S6D); however, the FANCL-independent FANCI monoubiquitination was not affected (Figure S6D).[12] These results are well explained by the specific disruption of the FANCL-UBE2T interaction by the p.Gln2Glu substitution.

In conclusion, we propose that *UBE2T* (*FANCT*) mutations define a FA subtype. This is also a rare example of a mutated E2 enzyme causing an inherited human disorder, like *UBE2A*.[20] The p.Gln2Glu substitution is probably hypomorphic, as indicated by the fact that a siUBE2T knockdown made AP65P-hTERT cells more sensitive to

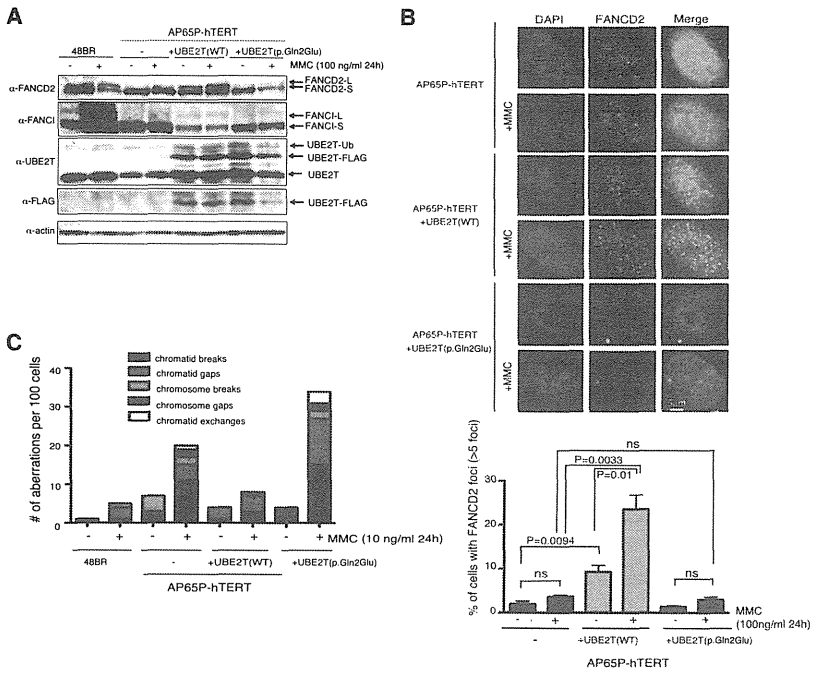

Figure 2. Functional Characterization of the Mutant UBE2T Protein

(A) Immunoblotting of cell lysates from normal fibroblasts (48BR) and from PNGS-252 (AP65P-hTERT) with or without indicated lentiviral transduction. AP65P primary fibroblasts (designated KURB1562 in JCRB) were obtained from the JCRB Cell Bank and transduced with an hTERT expressing retroviral vector pMSCV-hTERT-puro. For lentiviral production, HEK293T cells were transfected with CSII-CMV-MCS-IRES2-Bsd encoding human UBE2T-FLAG (either wild-type or the p.Gln2Glu mutant) together with packaging plasmids pCAG-HIVgp and pCMV-VSV-G-RSV-Rev, using Lipofectamine 2000. After 48 hr in culture, the 293T supernatants were filtered and added to the sparsely seeded AP65P-hTERT cells. Blastocidin S selection was started 2 days later (3 μg/ml). For immunoblotting, collected cells were lysed in RIPA buffer (50 mM Tris-HCl [pH 7.5], 150 mM NaCl, 0.5% sodium deoxycholate, 0.1% SDS, 1% NP-40, 5 mM EDTA, 20 mM β-glycerophosphate, 50 mM NaF, 1× protease inhibitor [Complete EDTA-free tablet Roche], 50 U/ml Benzonase, 1 mM PMSF). Samples were separated by SDS-polyacrylamide gel electrophoresis, transferred to a membrane, and detected with indicated antibodies and ECL reagents (GE Healthcare) using a LAS4000 Mini apparatus (GE Healthcare). The antibodies used in this study are summarized in Table S3.

(B) FANCD2 foci formation. Cells were grown on coverslips and subjected to 100 ng/ml MMC for 24 hr. Cells were then permeabilized with 0.5% Triton X-100/PBS for 10 min on ice and fixed with 3% paraformaldehyde/2% sucrose at room temperature for 30 min followed by blocking with 2% BSA/0.05% Triton X-100/PBS for 30 min at room temperature and staining with primary antibodies diluted in PBS containing 2% BSA and 0.05% Triton X-100 overnight at 4°C. Primary antibodies were detected by anti-rabbit Alexa 488 (Molecular Probes). Nuclei were stained with Prolong Gold mounting agent (Life Tech). Immunofluorescence images were captured with Keyence Biorevo BZ-9000. The mean and SD from three independent experiments are shown.

(C) Number of chromosomal aberrations induced by MMC treatment. MMC-exposed cells (10 ng/ml for 24 h) were arrested at M phase with Colcemid (100 ng/ml) for 3 hr, harvested, and further treated with 2 ml hypotonic 0.9% sodium citrate for 22 min. Carnoy's solution (4 ml) was added, followed by centrifugation at 1,200 rpm for 10 min. Cell pellets were washed once with 10 ml Carnoy's solution and resuspended in 1 ml Carnoy's solution. In each condition, 100 cells were scored.

MMC and completely eliminated the trace FANCD2 monoubiquitination that could still be observed in the siLuc control knockdown cells (Figures 3B and 3C). Finally, it is interesting to note a recent report suggesting that *UBE2T* functions with an unknown E3 in nucleotide excision repair.[21] It is common for an E2 to function with a set of E3 ligases, since far fewer E2s (~38) are encoded in the genome than E3 ligases (600–1,000).[22] UBE2T might have a partner other than FANCL, such as BRCA1[23] or other E3s, as has been suggested by yeast two-hybrid assays,[24,25] raising the possibility that UBE2T might have a function outside the FA pathway. Although a siUBE2T knockdown in AP65P-hTERT modestly sensitized cells to UV (Figure 3C), we detected only a marginal impact of *UBE2T* lentiviral transduction on UV survival (Figure 3D). These results suggest that the p.Gln4Glu substitution is a separation of function alteration that specifically reduces *UBE2T* function in the FA pathway but not in UV resistance. In line with this, neither of our FA-T-affected individuals experienced any photosensitivity. It thus remains unclear whether or how complete loss of *UBE2T* function would impact human phenotypes.

Accession Numbers

The WES sequencing data have been deposited in the European Genome-Phenome Archive (EGA) under the accession number EGA: EGAS00001001103.

Supplemental Data

Supplemental Data include case reports, six figures, and three tables and can be found with this article online at http://dx.doi.org/10.1016/j.ajhg.2015.04.022.

Acknowledgments

The use of *FANCT* as an alias for *UBE2T* was approved by the HUGO Gene Nomenclature Committee. We would like to thank the individuals PNGS-252 and -255 and their family members for making this work possible. We also thank Dr. Masao S. Sasaki (Professor Emeritus, Kyoto University) for his long-standing effort to collect Japanese FA samples, including AP65P fibroblasts; Dr. James Hejna (Graduate School of Biostudies, Kyoto University) for critical reading of the manuscript and English editing; Dr. Takayuki Yamashita (Gunma University) for GM6914 cells; Dr. Hiroyuki Miyoshi (RIKEN, currently at Keio University) and

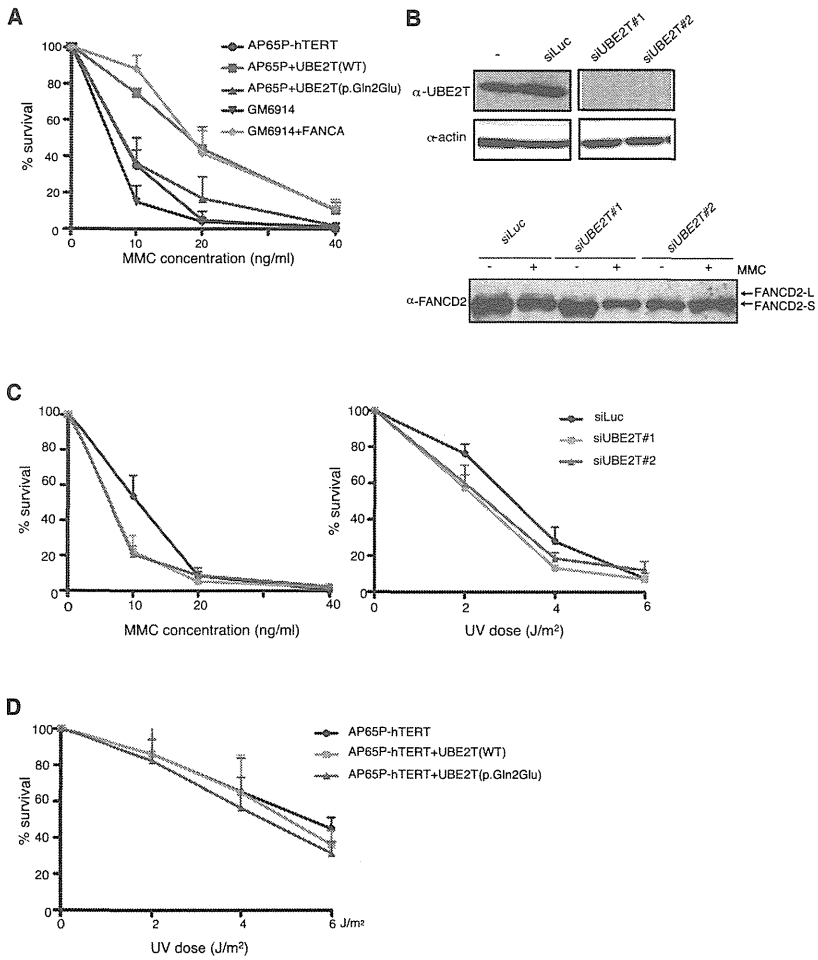

Figure 3. Cell Survival Curves after MMC or UV Treatment

(A) MMC sensitivity assay. AP65P-hTERT cells were exposed to varying concentrations of MMC for 24 hr, washed, and seeded into 6-well plates. After 5–7 days, surviving cells were counted using a LUNA digital automated cell counter (Logos Biosystems) or stained with 0.006% crystal violet/25% methanol solution. GM6914 (FA-A) and its complemented cells were included as control.

(B) Immunoblotting using the indicated antibodies (listed in Table S3). AP65P-hTERT cells were transfected with control (siLuc) or siRNAs targeting UBE2T (siUBE2T#1 and #2) (final 10 nM), seeded, and treated with MMC for 24 hr or UV irradiated. siRNAs (sequence listed in Table S2) were synthesized by Life Technologies and transfected using Lipofectamine RNAiMAX.

(C) MMC or UV sensitivity in AP65P-hTERT cells depleted of mutated UBE2T protein.

(D) UV sensitivity in AP65P-hTERT cells with or without UBE2T lentiviral transduction. The sensitivity assays were repeated at least three times, and a representative dataset with mean and SD of the triplicate cultures is shown.

RIKEN Bio-resource Center (Tsukuba, Ibaragi, Japan) for a lentivirus construct (CSII-CMV-MCS-IRES-Bsd) and the packaging system; Dr. Settara C. Chandrasekharappa (NIH) for advice on the CGH array; Dr. Yoko Katsuki for advice on immunofluorescence; Ms. Tomoko Hirayama (JCRB) for a protocol for karyotyping in fibroblasts; Ms. Fumiko Tsuchida, Chinatsu Ohki, Akiko Watanabe, and Mao Hisano for expert technical help; and Drs. Toshiyasu Taniguchi and Agata Smogorzewska for advice on anti-FANCD2/FANCI immunoblotting. The AP65P cell line (KURB1562) was kindly provided by JCRB Cell Bank, National Institute of Biomedical Innovation (Saito, Ibaraki, Osaka). This work was supported in part by grants from the Ministry of Health, Labor and Welfare of Japan.

Received: February 11, 2015
Accepted: April 30, 2015
Published: June 4, 2015

Web Resources

The URLs for data presented herein are as follows:

European Genome-phenome Archive (EGA), https://www.ebi.ac.uk/ega
Human Genetic Variation Database (HGVD), http://www.genome.med.kyoto-u.ac.jp/SnpDB/
NHLBI Exome Sequencing Project (ESP) Exome Variant Server, http://evs.gs.washington.edu/EVS/
OMIM, http://www.omim.org/
PolyPhen-2, http://www.genetics.bwh.harvard.edu/pph2/
RefSeq, http://www.ncbi.nlm.nih.gov/RefSeq
SIFT, http://sift.bii.a-star.edu.sg/

References

1. Alter, B.P. (2007). Diagnosis, genetics, and management of inherited bone marrow failure syndromes. Hematology (Am Soc Hematol Educ Program) *2007*, 29–39.
2. Kottemann, M.C., and Smogorzewska, A. (2013). Fanconi anaemia and the repair of Watson and Crick DNA crosslinks. Nature *493*, 356–363.
3. Walden, H., and Deans, A.J. (2014). The Fanconi anemia DNA repair pathway: structural and functional insights into a complex disorder. Annu. Rev. Biophys. *43*, 257–278.
4. Langevin, F., Crossan, G.P., Rosado, I.V., Arends, M.J., and Patel, K.J. (2011). Fancd2 counteracts the toxic effects of naturally produced aldehydes in mice. Nature *475*, 53–58.
5. Garaycoechea, J.I., Crossan, G.P., Langevin, F., Daly, M., Arends, M.J., and Patel, K.J. (2012). Genotoxic consequences of endogenous aldehydes on mouse haematopoietic stem cell function. Nature *489*, 571–575.

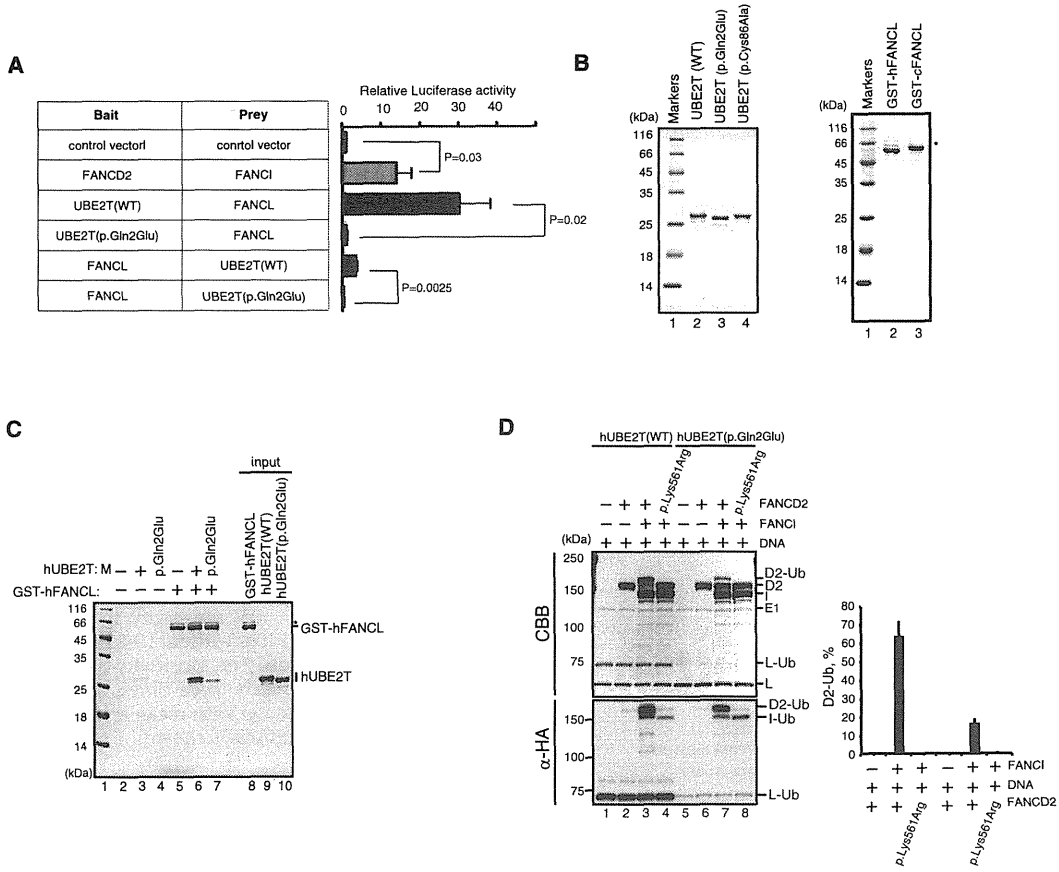

Figure 4. Functional Interaction between FANCL and UBE2T

(A) Mammalian two-hybrid assay. The assays were carried out as described.[19] In brief, *UBE2T* and *FANCL* in the bait vector (pM) or prey vector (pVP16) were co-transfected into 293T cells with the reporter luciferase vector as well as an internal control (pRL Renilla Luciferase vector). Luminescence signals were quantified using a Dual-Glo Luciferase Reporter Assay System (Promega). The signal was first normalized to transfection efficiency using Renilla luciferase levels and further divided by the value obtained by the empty bait and prey vector. The mean and SD of more than three independent experiments are shown. Statistical analysis was done using Student's t test, and p values are indicated.

(B) Purified recombinant proteins detected by Coomassie brilliant blue (CBB) gel staining. Human UBE2T proteins with or without the p.Gln2Glu substitution were produced in *E. coli* and purified to homogeneity as previously described.[11] WT, wild-type.

(C) In vitro pull-down assay between GST-human (h)FANCL and hUBE2T protein with or without the p.Gln2Glu substitution. Purified human UBE2T (6 μg) and GST-chicken FANCL or human FANCL (9 μg) were incubated at 37°C for 1 hr in 200 μl of reaction buffer containing 20 mM Tris-HCl (pH 7.5), 10% glycerol, 100 mM NaCl, 1 mM ZnOAc, 0.01% NP-40, and 5 mM 2-mercaptoethanol. Glutathione sepharose 4B beads (3 μl; GE Healthcare) were added to the reaction mixtures, and reaction mixtures were gently mixed at 25°C for 1 hr. The beads were then washed twice with 1 ml of reaction buffer. The proteins bound to the beads were separated by 15% SDS-PAGE and were visualized by Coomassie brilliant blue staining. Asterisk indicates read-through products.

(D) In vitro FANCD2 monoubiquitination assay in the presence of DNA. The assay was repeated three times, and the mean and SD of the percent of monoubiquitinated FANCD2 (D2-Ub) are shown in the graph. Execution of the in vitro FANCD2 ubiquitination reaction was as described.[11] As a control, FANCD2 protein carrying a p.Lys561Arg substitution blocking monoubiquitination was included. CBB, Coomassie brilliant blue. Immunoblotting with anti-HA (α-HA) was used to detect HA-tagged ubiquitin.

6. Lim, E.T., Würtz, P., Havulinna, A.S., Palta, P., Tukiainen, T., Rehnström, K., Esko, T., Mägi, R., Inouye, M., Lappalainen, T., et al.; Sequencing Initiative Suomi (SISu) Project (2014). Distribution and medical impact of loss-of-function variants in the Finnish founder population. PLoS Genet. *10*, e1004494.
7. Machida, Y.J., Machida, Y., Chen, Y., Gurtan, A.M., Kupfer, G.M., D'Andrea, A.D., and Dutta, A. (2006). UBE2T is the E2 in the Fanconi anemia pathway and undergoes negative autoregulation. Mol. Cell *23*, 589–596.
8. Alpi, A.F., Pace, P.E., Babu, M.M., and Patel, K.J. (2008). Mechanistic insight into site-restricted monoubiquitination of FANCD2 by Ube2t, FANCL, and FANCI. Mol. Cell *32*, 767–777.
9. Alpi, A., Langevin, F., Mosedale, G., Machida, Y.J., Dutta, A., and Patel, K.J. (2007). UBE2T, the Fanconi anemia core complex, and FANCD2 are recruited independently to chromatin: a basis for the regulation of FANCD2 monoubiquitination. Mol. Cell. Biol. *27*, 8421–8430.
10. Rajendra, E., Oestergaard, V.H., Langevin, F., Wang, M., Dornan, G.L., Patel, K.J., and Passmore, L.A. (2014). The genetic and biochemical basis of FANCD2 monoubiquitination. Mol. Cell *54*, 858–869.
11. Sato, K., Toda, K., Ishiai, M., Takata, M., and Kurumizaka, H. (2012). DNA robustly stimulates FANCD2 monoubiquitylation in the complex with FANCI. Nucleic Acids Res. *40*, 4553–4561.

12. Longerich, S., Kwon, Y., Tsai, M.-S., Hlaing, A.S., Kupfer, G.M., and Sung, P. (2014). Regulation of FANCD2 and FANCI monoubiquitination by their interaction and by DNA. Nucleic Acids Res. *42*, 5657–5670.
13. Longerich, S., San Filippo, J., Liu, D., and Sung, P. (2009). FANCI binds branched DNA and is monoubiquitinated by UBE2T-FANCL. J. Biol. Chem. *284*, 23182–23186.
14. Hira, A., Yabe, H., Yoshida, K., Okuno, Y., Shiraishi, Y., Chiba, K., Tanaka, H., Miyano, S., Nakamura, J., Kojima, S., et al. (2013). Variant ALDH2 is associated with accelerated progression of bone marrow failure in Japanese Fanconi anemia patients. Blood *122*, 3206–3209.
15. Hodson, C., Purkiss, A., Miles, J.A., and Walden, H. (2014). Structure of the human FANCL RING-Ube2T complex reveals determinants of cognate E3-E2 selection. Structure *22*, 337–344.
16. Butturini, A., Gale, R.P., Verlander, P.C., Adler-Brecher, B., Gillio, A.P., and Auerbach, A.D. (1994). Hematologic abnormalities in Fanconi anemia: an International Fanconi Anemia Registry study. Blood *84*, 1650–1655.
17. McVey, M., and Lee, S.E. (2008). MMEJ repair of double-strand breaks (director's cut): deleted sequences and alternative endings. Trends Genet. *24*, 529–538.
18. Yamada, T., Tachibana, A., Shimizu, T., Mugishima, H., Okubo, M., and Sasaki, M.S. (2000). Novel mutations of the FANCG gene causing alternative splicing in Japanese Fanconi anemia. J. Hum. Genet. *45*, 159–166.
19. Unno, J., Itaya, A., Taoka, M., Sato, K., Tomida, J., Sakai, W., Sugasawa, K., Ishiai, M., Ikura, T., Isobe, T., et al. (2014). FANCD2 binds CtIP and regulates DNA-end resection during DNA interstrand crosslink repair. Cell Rep. *7*, 1039–1047.
20. Nascimento, R.M.P., Otto, P.A., de Brouwer, A.P.M., and Vianna-Morgante, A.M. (2006). UBE2A, which encodes a ubiquitin-conjugating enzyme, is mutated in a novel X-linked mental retardation syndrome. Am. J. Hum. Genet. *79*, 549–555.
21. Kelsall, I.R., Langenick, J., MacKay, C., Patel, K.J., and Alpi, A.F. (2012). The Fanconi anaemia components UBE2T and FANCM are functionally linked to nucleotide excision repair. PLoS ONE *7*, e36970.
22. Ye, Y., and Rape, M. (2009). Building ubiquitin chains: E2 enzymes at work. Nat. Rev. Mol. Cell Biol. *10*, 755–764.
23. Ueki, T., Park, J.-H., Nishidate, T., Kijima, K., Hirata, K., Nakamura, Y., and Katagiri, T. (2009). Ubiquitination and downregulation of BRCA1 by ubiquitin-conjugating enzyme E2T overexpression in human breast cancer cells. Cancer Res. *69*, 8752–8760.
24. Sheng, Y., Hong, J.H., Doherty, R., Srikumar, T., Shloush, J., Avvakumov, G.V., Walker, J.R., Xue, S., Neculai, D., Wan, J.W., et al. (2012). A human ubiquitin conjugating enzyme (E2)-HECT E3 ligase structure-function screen. Mol. Cell. Proteomics *11*, 329–341.
25. van Wijk, S.J.L., de Vries, S.J., Kemmeren, P., Huang, A., Boelens, R., Bonvin, A.M.J.J., and Timmers, H.T.M. (2009). A comprehensive framework of E2-RING E3 interactions of the human ubiquitin-proteasome system. Mol. Syst. Biol. *5*, 295.

The American Journal of Human Genetics
Supplemental Data

Mutations in the Gene Encoding the E2 Conjugating Enzyme UBE2T Cause Fanconi Anemia

Asuka Hira, Kenichi Yoshida, Koichi Sato, Yusuke Okuno, Yuichi Shiraishi, Kenichi Chiba, Hiroko Tanaka, Satoru Miyano, Akira Shimamoto, Hidetoshi Tahara, Etsuro Ito, Seiji Kojima, Hitoshi Kurumizaka, Seishi Ogawa, Minoru Takata, Hiromasa Yabe, and Miharu Yabe

Supplemental Note: Case Reports

Individual 1 (PNGS-252) was born to unrelated healthy parents at 40 weeks with a birth weight of 2030 g (68% of the standard weight of Japanese babies). Upon delivery, a left hypoplastic thumb and abnormalities of external genitalia were noted. Short stature (-2 S.D.) was observed during her growth periods. She received pollicization at age 7 years, and preoperative blood counts revealed thrombocytopenia (Platelets 3.8 $x10^4$ per μl). A chromosomal breakage study with diepoxybutatane (DEB) showed an increased rate of chromosomal breakage of 0.48 per cell (normal range 0–0.07; Fanconi anemia range 0.3–12.0) confirming the diagnosis of Fanconi anemia. She developed severe pancytopenia, and required blood transfusions. She received bone marrow transplantation (BMT) from an HLA-matched unrelated donor at age 13, and remains alive in hematological remission after transplant.

Individual 2 (PNGS-255) was the only son of unrelated, healthy parents, and born at 40 weeks with a birth weight of 2600 g (84% of the standard weight of Japanese babies). Bilateral thumb polydactyly, abnormal shape of the left ear and left facial nerve palsy due to dysplasia of the middle ear bone was observed at birth. When he suffered from measles at age 3 years, anemia and thrombocytopenia were detected (Hb 6.8 g/dl, Platelets 4.3 $x10^4$ per μl). He was diagnosed with refractory anemia (RA) evolving to AML on the basis of findings from a bone marrow examination. Cytogenetic analysis of bone marrow revealed complex karyotypes with a 3q abnormality. A chromosomal breakage test with DEB showed an increased rate of chromosomal breakage (0.91 per cell). He developed acute myeloid leukemia, and received a BMT from an HLA-mismatched related donor at age 8. Hematological recovery was very poor, and he died of severe viral infection 5 months after BMT. He did not have a family history of any hematological disorder.

Supplemental data

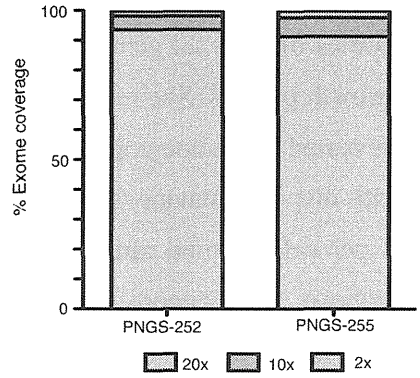

Figure S1. Exome coverage of genome samples from PNGS-252 and PNGS-255.
WES was carried out as previously described[1].

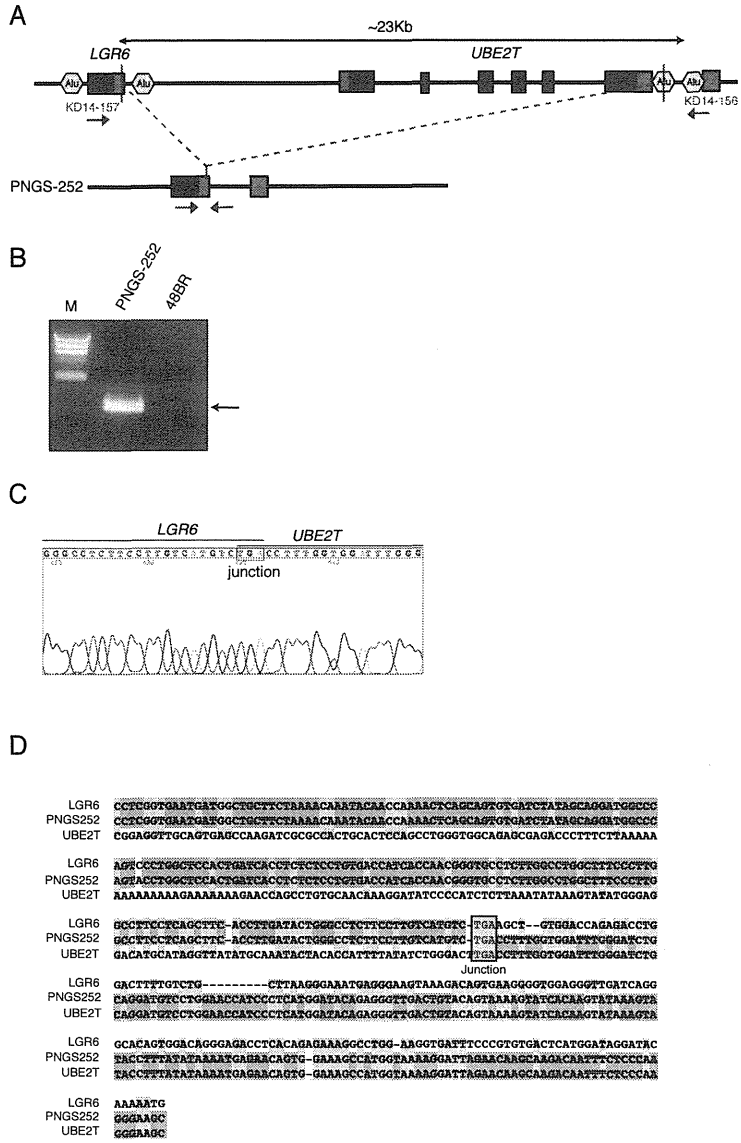

Figure S2. Large genomic deletion in the patient PNGS-252.

(A) A diagram depicting *UBE2T* and adjoining *LGR6* loci, Alu elements (yellow hexagons), and primer locations to detect the genomic deletion. Green boxes and black boxes indicate coding sequence and untranslated regions, respectively.

(B) Genomic PCR of indicated samples.

(C) Sanger sequencing chromatogram of the genomic PCR product across the junction point.

(D) An alignment of the sequences surrounding two breakpoints (in *LGR6* gene or *UBE2T* gene) and the fused sequence in PNGS-252 created by GENETYX-MAC

version 16. The red fonts indicate the junction with 3-bp microhomology (TGA). Identical residues across three or two sequences are indicated by yellow or blue colors, respectively.

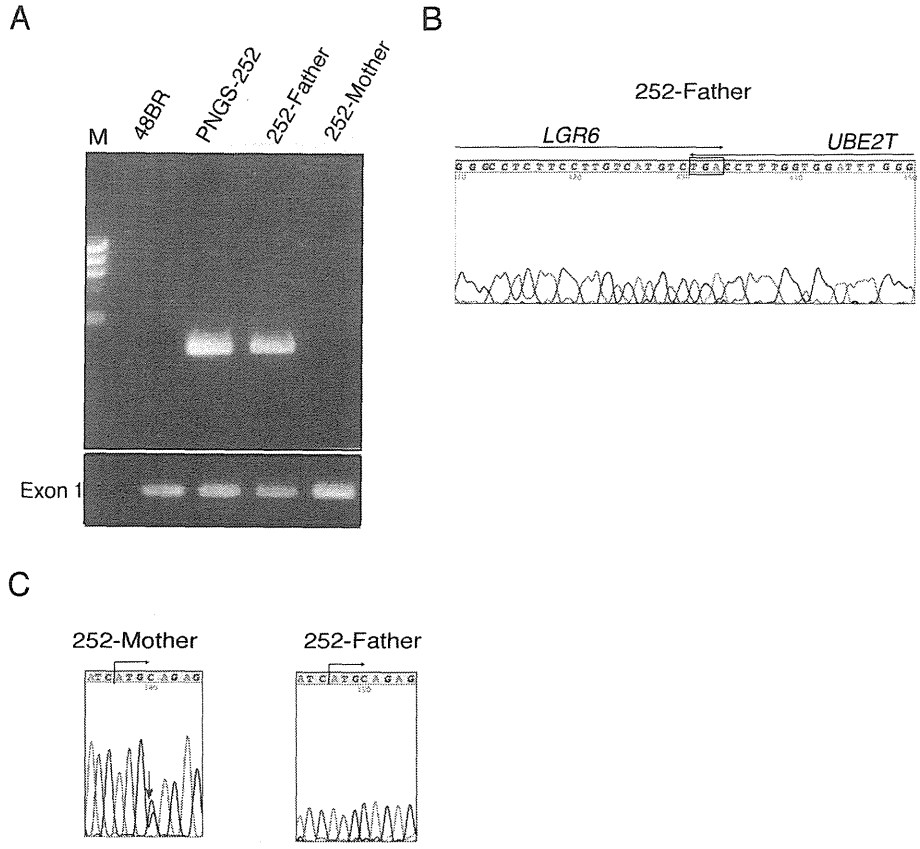

Figure S3. UBE2T mutation/deletion found in parents of PNGS-252.

(A) Genomic PCR to detect the *UBE2T* deletion as in Figure S2. PCR of *UBE2T* exon 1 serves as a positive control.

(B) Sanger sequencing chromatogram of the deletion junction in the sample from the father.

(C) Chromatogram of the direct sequencing. The c.C4>G mutation was detected only in the mother, not in the father, of PNGS-252.

A

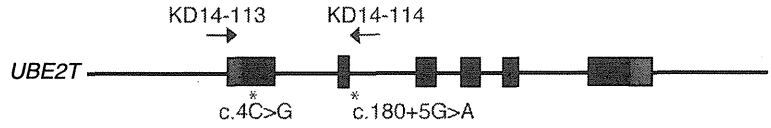

B

Colony	c.C4>G	c.180+5G>A
1	-	+
2	-	+
3	-	+
4	-	+
5	+	-
6	+	-
7	-	-
8	+	+

Figure S4. Two mutations found in PNGS-255 reside on different chromosomes.
To test if the c.C4>G mutation and the splice site mutation were allelic in PNGS-255, genomic DNA was PCR amplified using primers indicated in (A) (Table S2), cloned as a XhoI/NotI fragment into pBluescript, and sequenced. The results are shown in (B).

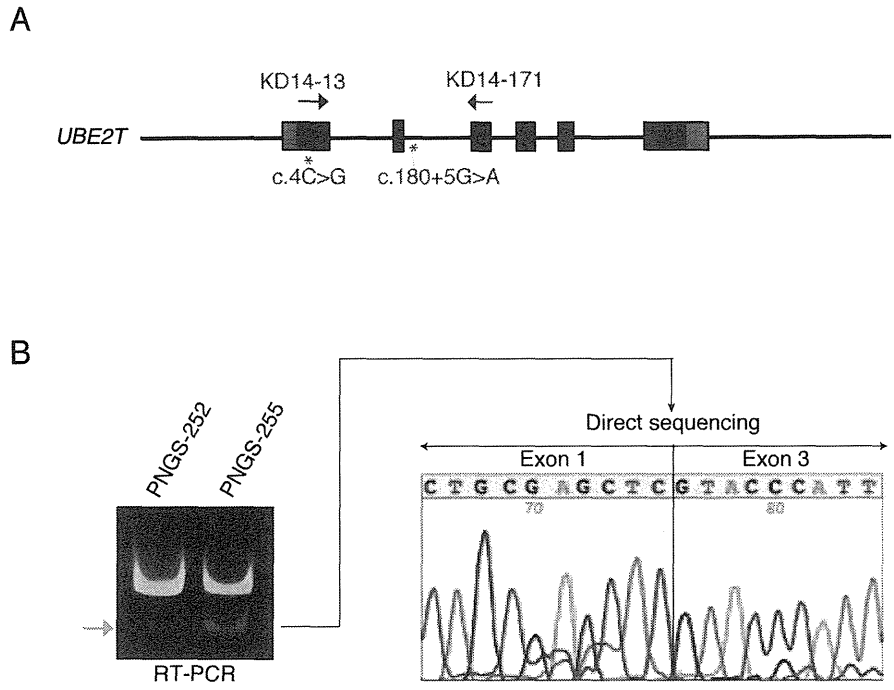

Figure S5. The effects of the splice site mutation in PNGS-255.

(A) Primer locations used for RT-PCR are indicated.

(B) UBE2T RT-PCR. Total RNA was isolated from bone marrow fibroblasts using an RNAeasy (Qiagen) kit. cDNA was synthesized with Superscript II VILO reaction mix (Life Technologies). UBE2T cDNA from the patient cells showed an additional faster migrating band in PNGS-255 but not in a PNGS-252 sample. The band was excised and eluted DNA was directly sequenced, revealing the skipping of exon 2 (right chromatogram).

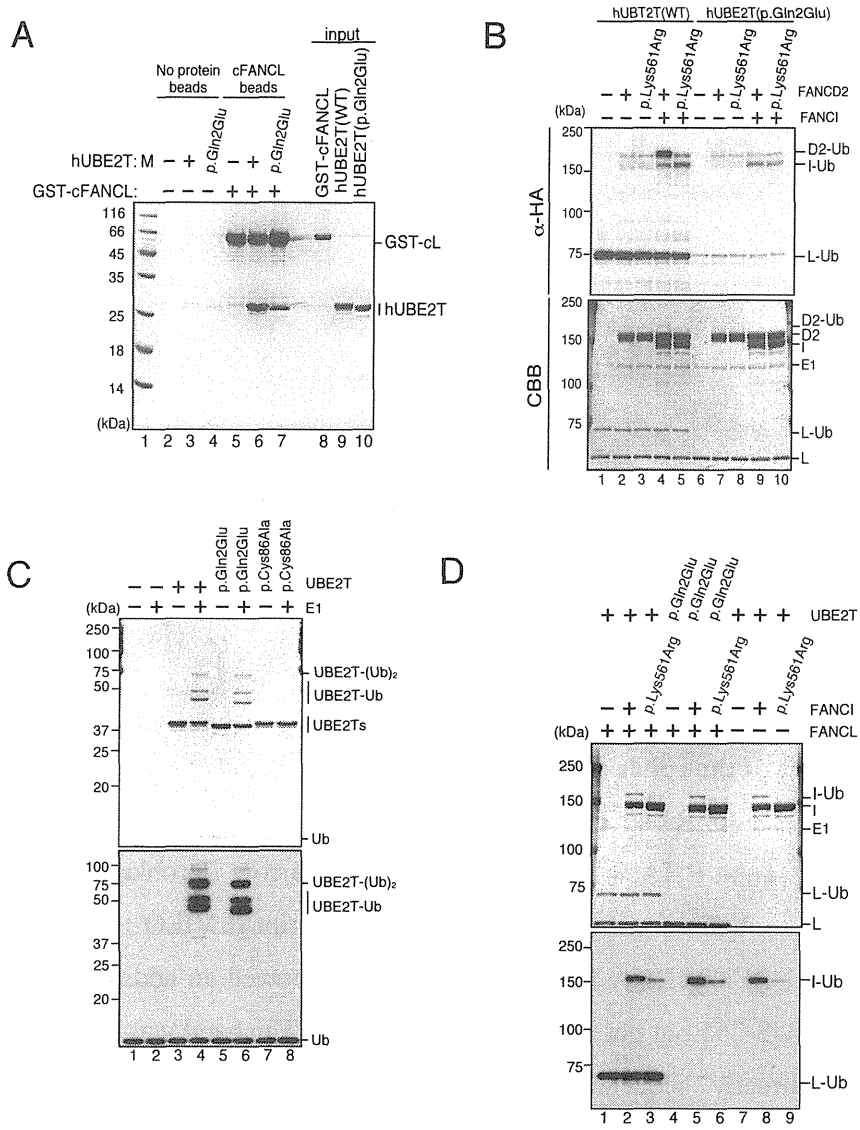

Figure S6. Recombinant UBE2T protein purification and *in vitro* assays. Ub, ubiquitin; WT, wild type.

(A) *In vitro* pull-down assay between GST-chicken FANCL (GST-cFANCL) and human (h) UBE2T protein with or without the p.Gln2Glu alteration.

(B) *In vitro* FANCD2 monoubiquitination assay in the absence of DNA.

(C) UBE2T autoubiquitination assay in the absence of FANCL.

(D) FANCL-independent FANCI monoubiquitination assay. Western blotting with anti-HA (a-HA) was used to detect HA-tagged ubiquitin.

Table S1. DNA primer sequences

Name	Sequences	Used for
KD14-13	ATGCAGAGAGCTTCACGTCTGAAGAGAGAG	UBE2T RT-PCR
KD14-171	TTTTGGTGGCAATTTGAGAACATCCAGACA	
KD13-3	ACTACATTGAAGCTGTTTGCTGAAAACTTC	c.C4>G validation, and UBE2T exon 1 PCR
KD13-4	GGTAGGGCACTCTGACCTTATAACTGCTCT	
KD14-156	TCCCCTCAGTGACCCTCATCTCCTGTCAGC	Detection of deletion junction in PNGS-252 and parents.
KD14-157	TCCAAACCCACGTTTCGTTCATTAATTATC	
KD14-113	AAAGCGGCCGCTTATGGTCACCTCTTTTCTC CTCCAGTGCA	Genomic PCR to determine whether two mutations in PNGS-255 were on the same chromosome or not.
KD14-114	AACTCGAGACCTAGTCCTTTATGCACTATCT ACTACAT	

Table S2. siRNA oligonucleotide sequences

Name	Sequence
siLuc	CGUACGCGGAAUACUUCGA
siUBE2T #1	GAAGAGAGAGCUGCACAUGUU
siUBE2T #2	UCAAGGUAGGCAACUUAGAUC

Table S3. Antibodies used in this study

Name	Type of antibody	Company	Catalogue number	Used for	Dilution
anti-FANCD2	rabbit, polyclonal	NB100-182	Novus Biologicals	Immunofluo-rescence	1:1000
anti-FANCD2	mouse, monoclonal	sc-20022	Santa Cruz Biotechnology	Western blotting	1:500
anti-UBE2T/HSPC150	rabbit, polyclonal	10105-2-AP	Proteintech	Western blotting	1:666
anti-FLAG M2	mouse, monoclonal	F3165	Sigma	Western blotting	1:1000
anti-FANCI	mouse, monoclonal	sc-271316	Santa Cruz Biotechnology	Western blotting	1:500
anti-HA (HA-probe)	mouse, monoclonal	sc-7392	Santa Cruz Biotechnology	Western blotting	1:333
anti-actin (20-33)	rabbit, polyclonal,	A5060	Sigma	Western blotting	1:400

References

1. Hira, A., Yabe, H., Yoshida, K., Okuno, Y., Shiraishi, Y., Chiba, K., Tanaka, H., Miyano, S., Nakamura, J., Kojima, S., et al. (2013). Variant ALDH2 is associated with accelerated progression of bone marrow failure in Japanese Fanconi anemia patients. Blood *122*, 3206–3209.

bjh research paper

Loss of function mutations in *RPL27* and *RPS27* identified by whole-exome sequencing in Diamond-Blackfan anaemia

RuNan Wang,[1] Kenichi Yoshida,[2,3] Tsutomu Toki,[1] Takafumi Sawada,[4] Tamayo Uechi,[4] Yusuke Okuno,[2,3] Aiko Sato-Otsubo,[2,3] Kazuko Kudo,[5] Isamu Kamimaki,[6] Rika Kanezaki,[1] Yuichi Shiraishi,[7] Kenichi Chiba,[7] Hiroko Tanaka,[8] Kiminori Terui,[1] Tomohiko Sato,[1] Yuji Iribe,[9] Shouichi Ohga,[10] Madoka Kuramitsu,[11] Isao Hamaguchi,[11] Akira Ohara,[12] Junichi Hara,[13] Kumiko Goi,[14] Kousaku Matsubara,[15] Kenichi Koike,[16] Akira Ishiguro,[17] Yasuhiro Okamoto,[18] Kenichiro Watanabe,[19] Hitoshi Kanno,[9] Seiji Kojima,[20] Satoru Miyano,[7,8] Naoya Kenmochi,[4] Seishi Ogawa[2,3] and Etsuro Ito[1]

[1]Department of Paediatrics, Hirosaki University Graduate School of Medicine, Hirosaki, [2]Cancer Genomics Project, Graduate School of Medicine, The University of Tokyo, Tokyo, [3]Department of Pathology and Tumour Biology, Graduate School of Medicine, Kyoto University, Kyoto, [4]Frontier Science Research Centre, University of Miyazaki, Miyazaki, [5]Division of Haematology and Oncology, Shizuoka Children's Hospital, Shizuoka, [6]Department of Paediatrics, Saitama National Hospital, Wako, [7]Laboratory of DNA Information Analysis, Human Genome Centre, Institute of Medical Science, The University of Tokyo, [8]Laboratory of Sequence Analysis, Human Genome Centre, Institute of Medical Science, The University of Tokyo, [9]Department of Transfusion Medicine and Cell Processing, Tokyo Women's Medical University, Tokyo, [10]Department of Perinatal and Paediatric Medicine, Graduate School of Medical Sciences, Kyushu University, Fukuoka, [11]Department of Safety Research on Blood and Biological Products, National Institute of Infectious Diseases, [12]Department of Transfusion, Omori Hospital, Toho University, Tokyo, [13]Department of Haematology and Oncology, Osaka City General Hospital, Osaka, [14]Department of Paediatrics, University of Yamanashi, Kofu, [15]Department of Paediatrics, Nishi-Kobe Medical Centre,Kobe, [16]Department of Paediat-

Summary

Diamond-Blackfan anaemia is a congenital bone marrow failure syndrome that is characterized by red blood cell aplasia. The disease has been associated with mutations or large deletions in 11 ribosomal protein genes including *RPS7*, *RPS10*, *RPS17*, *RPS19*, *RPS24*, *RPS26*, *RPS29*, *RPL5*, *RPL11*, *RPL26* and *RPL35A* as well as *GATA1* in more than 50% of patients. However, the molecular aetiology of many Diamond-Blackfan anaemia cases remains to be uncovered. To identify new mutations responsible for Diamond-Blackfan anaemia, we performed whole-exome sequencing analysis of 48 patients with no documented mutations/deletions involving known Diamond-Blackfan anaemia genes except for *RPS7*, *RPL26*, *RPS29* and *GATA1*. Here, we identified a *de novo* splicing error mutation in *RPL27* and frameshift deletion in *RPS27* in sporadic patients with Diamond-Blackfan anaemia. *In vitro* knockdown of gene expression disturbed pre-ribosomal RNA processing. Zebrafish models of *rpl27 and rps27* mutations showed impairments of erythrocyte production and tail and/or brain development. Additional novel mutations were found in eight patients, including *RPL3L*, *RPL6*, *RPL7L1T*, *RPL8*, *RPL13*, *RPL14*, *RPL18A* and *RPL31*. In conclusion, we identified novel germline mutations of two ribosomal protein genes responsible for Diamond-Blackfan anaemia, further confirming the concept that mutations in ribosomal protein genes lead to Diamond-Blackfan anaemia.

Keywords: bone marrow failure, Diamond-Blackfan, genetic analysis, erythropoiesis, childhood.

First published online 25 November 2014
doi: 10.1111/bjh.13229

rics, Shinshu University School of Medicine, Matsumoto, [17]Division of Haematology, National Centre for Child Health and Development, Tokyo, [18]Department of Paediatrics, Kagoshima University, Kagoshima, [19]Department of Paediatrics, Graduate School of Medicine, Kyoto University, Kyoto, and [20]Department of Paediatrics, Nagoya University Graduate School of Medicine, Nagoya, Japan

Received 21 August 2014; accepted for publication 7 October 2014
Correspondence: Professor Etsuro Ito, Department of Paediatrics, Hirosaki University Graduate School of Medicine, 53 Honcho, Hirosaki 036-8562, Japan.
E-mail: eturou@cc.hirosaki-u.ac.jp

Professor Seishi Ogawa, Cancer Genomics Project, Graduate School of Medicine, The University of Tokyo, 7-3-1, Hongo, Bunkyo-ku, Tokyo 113-8654, Japan.
E-mail: sogawa-tky@umin.ac.jp

Diamond-Blackfan anaemia (DBA) is an inherited rare red blood cell aplasia that is characterized by normochromic macrocytic anaemia, reticulocytopenia and selective defects in erythroid progenitor cells in normocellular bone marrow. Patients usually present with anaemia in the first year of life, although there is a non-classical mild phenotype diagnosed later in life. Macrocytic anaemia is a prominent feature of DBA but the disease is also characterized by growth retardation and congenital anomalies, including craniofacial, upper limb/hand, cardiac and genitourinary malformations, that are present in approximately half of the patients. In addition, DBA patients have a predisposition to malignancies including acute myeloid leukaemia, myelodysplastic syndrome, colon carcinoma, osteogenic sarcoma and female genital cancer (Lipton *et al*, 2006; Vlachos *et al*, 2008, 2012; Ito *et al*, 2010).

DBA is associated with single, monoallelic, inactivating mutations in ribosomal protein (RP) genes. Except for rare germline *GATA1* mutations reported in two X-linked DBA families (Sankaran *et al*, 2012), all known causative mutations have involved RP genes. Approximately 20% of DBA patients are familial. However, most cases occur sporadically and have *de novo* mutations. In DBA, mutations in RP genes include *RPS7*, *RPS10*, *RPS17*, *RPS19*, *RPS24*, *RPS26* and *RPS29* (encoding RP for the small subunit) and *RPL5*, *RPL11*, *RPL26* and *RPL35A* (encoding RP for the large subunit). These mutations have been reported in up to 60% of DBA patients (Draptchinskaia *et al*, 1999; Gazda *et al*, 2006, 2008, 2012; Cmejla *et al*, 2007; Farrar *et al*, 2008; Doherty *et al*, 2010; Konno *et al*, 2010; Gerrard *et al*, 2013; Mirabello *et al*, 2014). To date, approximately 40% of patients have no known pathogenic mutation. In this study, we carried out whole-exome sequencing (WES) analysis of 48 patients without known causative mutations or deletions and found loss-of function mutations in the *RPS27* and *RPL27* genes.

Methods

Patient samples

Genomic DNA (gDNA) was extracted from peripheral blood leucocytes with the QIAamp DNA Blood Mini Kit (QIAGEN, Hilden, Germany) according to the manufacturer's protocol. The diagnosis of DBA was based on the criteria developed at an international clinical consensus conference (Vlachos *et al*, 2008). All clinical samples were obtained with informed consent from paediatric and/or haematology departments throughout Japan. The Ethics Committee of Hirosaki University Graduate School of Medicine and the University of Tokyo approved this study.

Whole-exome sequencing analysis

To identify the candidate disease variants including non-RP genes, we performed WES analysis. gDNA from patients was enriched for protein-coding sequences with a SureSelect Human All Exon V3, V4 or V5 kit (Agilent Technologies, Santa Clara, CA, USA). This was followed by massively